Available online at www.sciencedirect.com

ScienceDirect

Procedia CIRP 45 (2016) 279 – 282

www.elsevier.com/locate/procedia

3rd CIRP Conference on Surface Integrity (CIRP CSI)

Surface integrity of SA508 Gr 3 subjected to abusive milling conditions

A. Maurotto[a]*, Y. Gu[b], D. Tsivoulas[b,c], M.G. Burke[b]

[a]*Nuclear Advanced Manufacturing Research Centre, The University of Sheffield, Brunel Way, S60 5WG Catcliffe, U.K.*
[b]*Materials Performance Centre, School of Materials, The University of Manchester, Oxford Road, M13 9PL, Manchester, U.K.*
[c]*Amec Foster Wheeler, Clean Energy Europe, 601 Faraday Street, Birchwood Park, Warrington, WA3 6GN, UK*
** Corresponding author. Tel.: +44-114-215-8013. E-mail address: a.maurotto@sheffield.ac.uk*

Abstract

SA508 Gr 3, a bainitic forging steel employed in the fabrication of nuclear pressure vessels has been characterised after dry-milling to investigate extent of machining abuse on the surface. A detailed study of the evolution of residual stresses, microstructure, micro-hardness and roughness in relation to different milling parameters is presented. A central composite orthogonal (CCO) design of experiments (DoE) was used to generate a statistic model of the milling process. Deformation of the sub-surface layer was assessed via SEM BSE imaging. The developed statistical model is discussed aiming to illustrate availability of different cost-effective manufacturing techniques meeting the high standards required by the industry.

© 2016 The Authors. Published by Elsevier B.V. This is an open access article under the CC BY-NC-ND license (http://creativecommons.org/licenses/by-nc-nd/4.0/).

Peer-review under responsibility of the scientific committee of the 3rd CIRP Conference on Surface Integrity (CIRP CSI)

Keywords: Surface integrity; face milling; machinability; design of experiments.

1. Introduction

The systematic increase in world-wide demand for carbon-free energy has greatly augmented the pressure to the nuclear industry to consider ways to meet energy needs while maintaining environmental sustainability. Steels alone represent the majority of structural materials employed in light water reactors and low alloy steels such as SA508 Gr 3 are commonly used in the fabrication of pressure vessels. In this application they are used for extended times at maximum operating temperatures of 280 to 315 °C, and pressures between 7 and 15 MPa (respectively in BWR and PWR) [1]. Machinability of this steel is relatively good and significant experience has been developed over the years to solve machining problems caused by its high ductility, tensile strength and work-hardening ratio. New trends in the nuclear industry, however, are pushing the operational life of reactors to 60 years and beyond [2]. For such extended operation, surface defects resulting from the manufacturing process can influence fatigue, corrosion resistance and resistance to brittle fracture. Thus, surface integrity requirements can become even more stringent limits [3].

Nomenclature

a_p	depth-of-cut
f_z	feed per tooth
V_c	cutting speed
XRD	X-Ray Diffraction
SEM	Scanning Electron Microscope
BSE	Backscatter Electron
R_a	Arithmetic mean surface roughness
R_z	Mean roughness depth
DoE	Design of Experiments
RS	Residual stress

When the work-piece is subject to non-uniform deformations such as in the case of machining, locked-in stresses develop [4]. The material undergoes compressive deformation in front of the cutting edge and tensile deformation immediately after [5]. The deformation energy and friction release large amount of heat which adds to the undesired tensile stress field after cooling [6]. Bainitic steels, however, exhibit higher thermal conductivity coefficients when compared with austenitic stainless steels thus reducing the effect of the heat generated during cutting. The goal of the modern nuclear industry is to manufacture low-cost, high quality products in short time to drive down the associated costs. When compared

2212-8271 © 2016 The Authors. Published by Elsevier B.V. This is an open access article under the CC BY-NC-ND license (http://creativecommons.org/licenses/by-nc-nd/4.0/).
Peer-review under responsibility of the scientific committee of the 3rd CIRP Conference on Surface Integrity (CIRP CSI)
doi:10.1016/j.procir.2016.02.094

with other methods, hard milling produces excellent surface integrity while being cost effective. In the case of dry milling, additional good cleanliness and smoothness of the machined surface are expected.

Modeling the dry hard milling process can be used to implement a more efficient process. In this work, a statistical model, which considers the complex interrelation between machining parameters, is presented and material's response to challenging cutting conditions is investigated.

2. Experimental

The alloy studied in this work was a SA508 Grade 3 steel with chemistry presented in Table 1. Machining coupons were produced out of water-jet cut plates. Each coupon dimensions were 100x200x25 mm; the 100 mm sides were both machined and four responses were recorded: R_a, R_z, maximum residual stress and surface hardness. The dry machining process was performed in one pass, ensuring that a tool engagement of 80% was achieved. After each machining test, cutting inserts were inspected and replaced when any wear or damage was apparent since tool wear is known to significantly influence magnitude of surface deformation and thus the residual stresses [6].

Surface roughness was assessed with a Mitutoyo Surftest SJ-410 stylus on finished work-pieces. Residual stress measurements were performed by X-Ray Diffraction using a Proto iXRD combo residual stress analyser fitted with a Mn-K_α tube and operating at 20 kV and 4 mA.

The specimens were subsequently evaluated using a Zeiss Sigma VO field emission gun (FEG) – scanning electron microscope (SEM) operated at 20kV and equipped with an Oxford Instruments X-max 150 Silicon Drift Detector (SDD) energy dispersive x-ray spectrometer, with the Aztec analysis system. To quantify the extent of the deformed layer, BSE imaging analysis of the work-piece was performed on a metallographic cross-section specimen. Samples for BSE analysis were prepared via a standard metallographic procedure with a final stage of polishing with 0.02 µm colloidal silica.

Machining tests were performed on a 3-axis Mazak Vertical Venter Smart 430A using a Sandvik Coromill R300 tool head with 53 mm diameter, extra close pitch and five insert spaces. The indexable button insert selected for the experiments was a tungsten carbide, Ti(Al)N coated, Coromill R300-1240-1040 with a diameter of 12 mm.

Surface hardness measurements were obtained using a Vickers micro-indenter with 0.1 N load and a dwell time of 15 s.

Table 1: Chemical composition of the SA508 Gr 3 steel

Element	Fe	C	Si	Cr	Ni	Mn	Mo
Weight%	balance	0.23	0.31	0.3	0.85	0.75	0.6

A Box-Wilson (CCO) Design of Experiment was used to identify which cutting parameters had statistically significant influence on the responses and the interaction between them. The DoE incorporated three key process parameters: depth of cut a_p, feed per tooth f_z and cutting speed V_c. The relatively complex CCO design (Table 2) with three center points and no replicates allowed to accurately describe the system's response keeping into account the non-linearity and estimating the variability and repeatability of its response. Tests were randomized to minimize external influences into the measured responses and analysis of the results was carried out on Umetrics' Modde 11 software by using the Partial Least Square method.

Table 2: Experimental cutting parameters

Run order	V_c [m/min]	a_p [mm]	f_z [mm/th]
1	120	2.5	0.275
2	363	3.24	0.18
3	363	1.76	0.37
4	260	1.5	0.275
5	260	2.5	0.4
6	400	2.5	0.275
7	260	2.5	0.275
8	363	1.76	0.18
9	157	1.76	0.37
10	157	3.24	0.18
11	157	1.76	0.18
12	260	3.5	0.275
13	157	3.24	0.37
14	260	2.5	0.275
15	363	3.24	0.37
16	260	2.5	0.15
17	260	2.5	0.275
18	260	1.5	0.275

3. Results

Five different areas were selected on each machined surface and their surface roughness results averaged to reduce the influence of accidental damage or local inhomogeneity. The standard deviation of the results was used to evaluate the quality of the measure. Surface roughness remained good in the full experimental range even at cutting parameters that were significantly higher than the recommended values. Both the R_a and R_z appeared to change in a non-linear way when varying the key cutting parameters, sign of an interaction between the parameters.

All hardness test results showed limited scatter, averaging at 235±9 HV0.1-15, with good replicate match.

Surface XRD residual stress measurements were performed for seven areas, which were selected on the cut face of the sample. These results were then averaged to increase confidence in the measure and reduce the effects of surface quality or transient inhomogeneity in the cutting process. The measured stress appeared to decrease with a lower depth of cut a_p and increase with increasing V_c. It was interesting to note that the majority of data points fell in the region of ~450-550 MPa with only two measures reporting stresses slightly above it (586 and 625 MPa). The chance that those higher values were due to local inhomogeneity in the microstructure or in the surface of the samples was ruled out by performing several additional measurements on the surface and obtaining similar

stress values. Three of the samples were replicates; they exhibited good reproducibility of the process with maximum residual stress differing only by ~25 MPa, well below the experimental error.

Analysis of the experimental data was performed with the statistical software Modde 11, which was also used to generate the mathematical model.

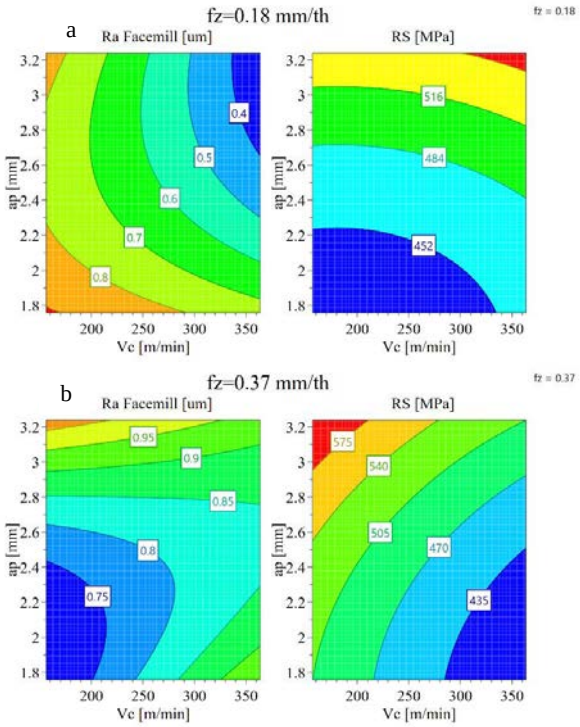

Figure 1:Contour plot for Ra and residual stress for low fz=0.18 mm/th (a) and high fz=0.37mm/th (b)

In Figure 1 contour plots are used to summarise a large amount of information obtained from the model developed. The top graphs in Figure 1a, corresponding to an f_z=0.18 mm, show how the surface roughness appeared to decrease with increasing cutting speed with almost no dependence on depth of cut. Rather, the surface stress increased rapidly with increased a_p, and cutting speed changes did not significantly influence the surface stress. Bottom graphs (Figure 1b) are corresponding to an f_z=0.37 mm. When comparing this case with the former it is evident that surface roughness exhibited a much more complex behavior. R_a appears to increase slightly with cutting speed up to an a_p=~2.8 mm, above this value it did not appear to depend any longer from the cutting speed but only increase with increasing depth of cut. Residual stress, instead, appeared to decrease with increasing cutting speed, and rapidly grow at higher a_p, similarly to what was observed at a lower feed per tooth.

The developed model exhibited a good fit for R_a R_z and residual stress with a statistical R^2 equal to 0.85, 0.79 and 0.86 respectively. Prediction power was acceptable for both R_a and R_z with a statistical Q^2 of 0.5 and 0.49 respectively, and good for residual stress (Q^2=0.65).

Figure 2 shows the machined surface of a SA508Gr3 steel milled at V_c=400 m/min, a_p=2.5 mm, f_z=0.275 mm. The surface topography shown by SEM imaging clearly reflected the cutting traces.

The effect of machining on the surface and sub-surface microstructures of this sample were examined using BSE imaging to assess the deformation through electron channeling contrast effects. In Figure 3, the BSE image shows the heavily-deformed surface layer consisting of ultra-fine grains which could not be shown at low magnification.

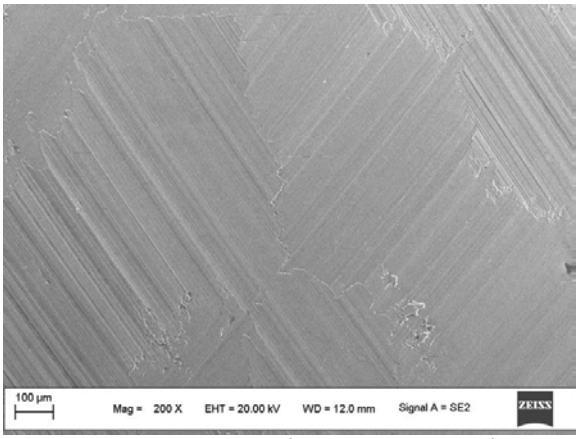

Figure 2: Secondary electron image of sample 6 showing the surface topography of the abusively machined surface of SA508 Gr 3 steel.

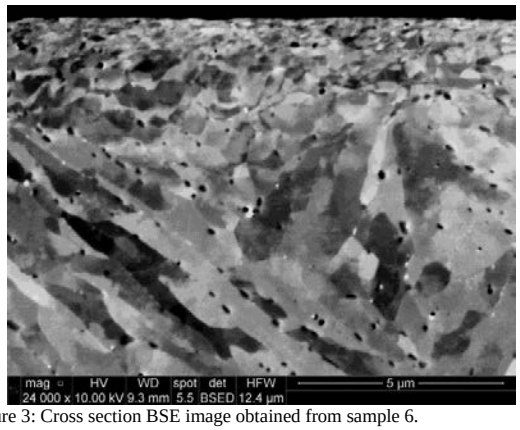

Figure 3: Cross section BSE image obtained from sample 6.

The depth of the deformed layer was about 5 µm as determined via BSE images, though the thickness of the layer was not strictly homogeneous in this case.

4. Discussion

The classical approach of having one-dimensional maps with data on a straight line (by fixing two variables while allowing the third to vary) fails to identify complex interaction between cutting parameters such as in this case. The wider coverage of the experimental space in the case of 2D parametric maps allows an easier identification of interactions among parameters and promotes a sounder optimization of cutting parameters. In this case, the interrelationship between cutting parameters generate a strongly non-linear response of the

system, not allowing the complete separation of the effect of each factor with respect to the others.

One noteworthy observation in the present work was that the measured hardness remained stable in respect to the process parameters. In Figure 3, the depth of deformed layer was approximately 5 µm. This depth was consistent in every sample analyzed and could explain the hardness results. Similarly, the measured responses in R_a showed noteworthy differences in their interaction with the cutting parameters. For the lower f_z=0.18 mm, R_a appeared to depend from a_p only up to about a_p=2.5 mm. Above that value only V_c was influencing it significantly. The unusual behavior of a_p could be explained by a change in the chip formation regimen, which became stable only for an a_p>2.5 mm. The higher f_z=0.37 mm exhibited for R_a an opposite behavior. In this case roughness became almost independent from V_c for a_p>2.8 mm. When comparing experimental runs at high and low f_z it was evident that surface roughness was negatively influenced by the increase in f_z as expected.

In terms of surface residual stresses, higher a_p and f_z exhibited detrimental effects by generating higher tensile stresses [Figure 1]. This is expected as the larger interaction volume between the tool and work-piece contributed to a thicker average chip and ultimately to higher cutting forces [8]. Larger cutting forces increase the extent of the plastic deformation gradient on the surface, leading to sharper differences between the deformed layer and the substrate, ultimately resulting in a higher magnitude stress field [9]. Similarly, higher heat generation associated with a thicker chip contributed, on cooling, to increasing the tensile residual stress field.

Interestingly, residual stresses appeared to decrease when V_c is increased. This could be explained in terms of the reduced time available for the heat generated in the cutting zone to dissipate into the work-piece. At higher speeds, a larger part of deformation heat is removed with the chip, thus lessening the contribution of temperature to the tensile stress field. On another note, the built-up edge formation could be the cause of the higher tensile field at lower cutting speeds [10]. An uncomplicated direct link between cutting speed, surface roughness and residual stresses is, however, not observed [11], as V_c appears to be strongly inter-dependent on the other machining parameters and different cutting regimens.

Microstructural analysis of the cross-section of the machined surfaces can provide information to aid in evaluating the depth of the deformed layer. However, the SA508 Grade 3 steel studied in this work is a bainitic steel (consistent with the microstructure revealed by BSE imaging in Figure 3), which is characterized by numerous lath and sub-grain boundaries. This complex microstructure may affect the assessment of the deformed layer thickness as measured via BSE imaging compared to machined austenitic stainless steels. It is, however, useful to point out that the deformation depth is generally low and comparable to these observed in a previous study [12].

5. Conclusions

A statistical model capable of understanding the complex interaction between process parameters in an extended range was developed from experimental results for dry milling. The measured hardness after machining, often the key parameter evaluated by industry, exhibited very limited variation in the full experimental range, remaining close to the hardness value of as-supplied material.

Although the roughness remained well-below the maximum allowed for this type of application ($R_a \leq 3.2$ µm), it exhibited a noteworthy behavior with respect to a_p especially for high f_z when it became independent of cutting speed V_c. This, coupled with the behavior observed for residual stresses indicate significant potential productivity benefits by running high performance cuts in dry milling of SA508.

The deformed layer thickness was observed to be small and did not appear to be influenced by the key cutting parameters in the full experimental range taken into account. Surface integrity remained high even at abusive cutting conditions.

With respect to residual stresses, the most evident trend was the reduction of stress for high performance cuts (high f_z and V_c) but a_p was to be maintained in a reduced range to take advantage of this behavior with the additional benefit of positively influencing R_a.

Acknowledgements

The authors would like to acknowledge Sandvik Coromant for tooling and assistance by their staff. Funding from the Engineering and Physical Sciences Research Council under the NNUMAN research program, grant number EP/J021172/1 is also acknowledged.

References

[1] Nanstad RK. In Bever MB editors. Encyclopedia of Material Science and Engineering, Pergamon, New York; 1986.
[2] Klueh RL, Nelson AT. Ferritic/martensitic steels for next-generation reactors, Journal of Nuclear Materials, 2007 vol 371, p. 37-52.
[3] Groover MP. Fundamental of Modern Manufacturing-Materials Processes and Systems, Prentice-Hall, Englewood Cliffs, NJ, 1990.
[4] Jang DY, Watkins TR,.Kozaczek KJ. Hubbard CR, Cavin OB. Wear, 1996 vol 194, p. 168-173.
[5]]Klocke F, Brinksmeier E, Weinert K. CIRP Annals Manufacturing Technology, 2005 vol 54, p.22-45.
[6] Tönshoff HK, Arendt C, Amor RB. CIRP Annals Manufacturing Technology, 2000 vol 49, p.547-566.
[7]] Eriksson L, Wold S. Design of Experiments: Principles and Applications, Umetrics Academy, Umeå, Sweden, 2008.
[8] Pathak BN, Sahoo KL, Mishra M. Materials and Manufacturing Processes, 2013 vol 28, p. 463-469.
[9] Ben Moussa N, Sidhom H, Braham C. International Journal of Mechanical Sciences, 2012 vol 64, p. 82-93.
[10] Gökkaya H, Strojniški vestnik. Journal of Mechanical Engineering, 2010 vol 56, p. 584-593.
[11] Shaw MC. Metal cutting principles, Oxford university press, Oxford, UK, 1997.
[12] Maurotto A, Tsivoulas D, Burke MG. Surface integrity in dry milling of 304L steel: A parametric study. Procedia CIRP, 2014 Vol. 13, p. 156-162.